

Differences in Ischemic Lesion Evolution in Different Rat Strains Using Diffusion and Perfusion Imaging

Juergen Bardutzky, MD; Qiang Shen, PhD; Nils Henninger, MD; James Bouley, BS;
Timothy Q. Duong, PhD; Marc Fisher, MD

Background and Purpose—Interstrain differences in the temporal evolution of ischemia after middle cerebral artery occlusion (MCAO) in rats may considerably influence the results of experimental stroke research. We investigated, in 2 commonly used rat strains (Sprague-Dawley [SD] and Wistar-Kyoto [WK]), the spatiotemporal evolution of ischemia after permanent suture MCAO using diffusion and perfusion imaging.

Methods—Serial measurements of quantitative cerebral blood flow (CBF) and apparent diffusion coefficient (ADC) were performed up to 210 min after MCAO. Lesion volumes were calculated by using previously established viability thresholds and correlated with infarct volume defined by 2,3,5-triphenyltetrazolium chloride staining 24 hours after MCAO.

Results—While the ADC-derived lesion volume increased rapidly during the first 120 min after MCAO and essentially stopped growing after 3 hours in SD rats, ADC lesion in WK rats increased progressively during the entire 210-min period and was significantly smaller at all time points ($P < 0.05$). The abnormal perfusion volume correlated highly with the TTC-defined infarct size in both groups. In WK rats, the abnormal perfusion volume was significantly larger than the abnormal diffusion volume up to 90 min after MCAO ($P < 0.001$), whereas the diffusion/perfusion mismatch was significant ($P < 0.001$) only at 45 min in SD rats. ADC-CBF scatterplots analysis revealed a slower and less robust ADC decline over time in WK rats in pixels with severe ($< 20\%$ of normal) and moderate (21 to 40% of normal) CBF reduction.

Conclusions—This study demonstrated substantial differences in acute ischemic lesion evolution between SD and WK rats. These interstrain variations must be taken into account when assessing new therapeutic approaches on ischemic lesion evolution in the rat MCAO model. (*Stroke*. 2005;36:2000-2005.)

Key Words: cerebral blood flow ■ diffusion-weighted imaging ■ focal ischemia ■ rat strains

Experimental models of stroke are essential to study the pathophysiology of cerebral ischemia and to evaluate the effects of novel therapeutic approaches. The intraluminal suture occlusion of the middle cerebral artery (MCAO) in rats is one of the most widely used models to study focal cerebral ischemia. However, considerable variability in the extent of final infarct size have been recurrent findings with this model^{1,2} and compromised its potential in preclinical therapeutic assessments. This may be explained by a number of factors, including differences in anesthesia, in size and type of filament used, and modifications of the technique.¹⁻³

Moreover, some studies have noticed strain-dependent differences in ischemic severity and extent of final infarction.^{4,5} However, all of these studies focused on the final infarct volume using classic histologic methods. None of these studies evaluated the in vivo evolution of the ischemic lesion during the acute phase, and it remains unclear whether the dynamics of the ischemic penumbra, the main target of acute stroke therapy,⁶ differs between different rat

strains. Interstrain discrepancies in neuroprotective efficiency reported by several studies^{4,7} may be explained by substantial differences in acute ischemic lesion evolution. Therefore, characterization of strain-specific spatial and temporal evolution of ischemia is desirable to adequately design, interpret, and compare studies on neuroprotection in focal cerebral ischemia in rats.

Diffusion- (DWI) and perfusion-weighted (PWI) magnetic resonance imaging (MRI) are powerful imaging modalities for early detection of cerebral ischemia and allow for noninvasive follow up of ischemia evolution with a reasonable temporal and spatial resolution.⁸ The region with perfusion abnormality, but without diffusion abnormality, referred to as the diffusion/perfusion mismatch, is thought to represent an approximation of the ischemic penumbra.⁶

The purpose of the present study was to investigate, in 2 commonly used rat strains, the spatial and temporal evolution of focal ischemia in the permanent suture model. Combined quantitative diffusion and perfusion imaging were used to detect the diffusion/perfusion mismatch during the acute stroke phase.

Received February 25, 2005; accepted May 19, 2005.

From the Department of Neurology (J.B., N.H.), University of Heidelberg, Heidelberg, Germany; Yerkes National Primate Research Center (Q.S., T.Q.D.), Emory University, Atlanta, Ga; and Department of Neurology (M.F.), Massachusetts Medical School (J.B.), Worcester, Mass.

Correspondence to Juergen Bardutzky, INF 40069120 Heidelberg, Germany. E-mail juergen_bardutzky@med.uni-heidelberg.de

© 2005 American Heart Association, Inc.

Stroke is available at <http://www.strokeaha.org>

DOI: 10.1161/01.STR.0000177486.85508.4d

Materials and Methods

Animal Preparation

Two different strains of rats were studied: male Wistar-Kyoto rats (WK; $n=9$, 324 ± 15 g, age: approximately 9 weeks, Taconic Farms, New York) and male Sprague-Dawley rats (SD; $n=9$, 314 ± 19 g, age: approximately 9 weeks, Taconic Farms, New York). After an overnight fast, anesthesia was induced with an intraperitoneal injection of chloral hydrate (400 mg/kg). PE-50 tubing was inserted into the right femoral artery for continuous monitoring of arterial blood pressure and heart rate (Biopac, Santa Barbara, Calif) throughout the study, and for measuring arterial pO_2 , pCO_2 , pH, and plasma glucose (I-STAT, Heska Corp.) at baseline and 4 hours after the induction of ischemia. Rectal temperature was monitored and kept at $37 \pm 0.5^\circ\text{C}$ throughout the entire study using a feedback-controlled heating pad.

Permanent focal cerebral ischemia was produced by intraluminal suture occlusion of the right MCAO using a 4–0 silicone-coated nylon filament as previously described.⁹ Once the animal was in the magnet, anesthesia was switched to 1% isoflurane delivered in air at 1.5 L/min.

Magnetic Resonance Imaging Measurements

MRI was performed on a Bruker 4.7T/40 cm horizontal magnet and a 20 G/cm magnetic field gradient insert. A surface coil was used for brain imaging and an actively decoupled neck coil was used for cerebral blood flow (CBF) labeling. Coil-to-coil electromagnetic interaction was actively decoupled.

The average apparent diffusion coefficient (ADC) of water was obtained by averaging 3 ADC maps acquired separately with diffusion-sensitive gradients applied along the x, y, or z direction. Single-shot, spin-echo echoplanar images (EPI) were acquired with a 64×64 matrix, 25.6×25.6 mm² field of view (FOV), 8 1.5-mm slices, TR=2 sec, b=10 and 1270 sec/mm², TE=37.5 ms, $\Delta=17.5$ ms, $\delta=5.6$ ms, and 16 averages (total acquisition time 2.5 min).

Noninvasive quantitative CBF measurements were carried out using the continuous arterial spin-labeling (ASL) technique.⁹ Paired images were acquired alternately, one with arterial spin-labeling and the other without spin-labeling preparation (control). Single-shot, gradient-echo EPI were acquired with identical parameters except TE=15 ms. For each set of CBF measurement, 120 pairs of images were acquired for signal averaging, with 60 pairs obtained before and 60 pairs after the ADC measurements (total acquisition time 8.9 min).

The postocclusion time quoted was at the middle of the MRI acquisition at each time point. Imaging was performed at 45, 90, 120, 180, and 210 min after occlusion.

Postmortem Evaluation

Twenty-four hours after ischemia, histologic staining was performed using 2,3,5-triphenyltetrazolium chloride (TTC). According to the MRI slices, brains were cut into 8 1.5-mm thick coronal slices starting 1 mm from the frontal pole. The stained sections were then photographed and infarct volumes were determined using ImageJ software (<http://rsb.info.nih.gov/ij/>). To compensate for the effects of brain edema, a corrected infarct volume was calculated as previously described.¹⁰

Data Analysis

Calculation of In Vivo Lesion Size

MRI measurements were analyzed using the imaging processing programs Matlab (Math-Works) and STIMULATE.¹¹ Quantitative CBF and ADC_{av} maps were calculated as previously described in details.⁹

In the same permanent ischemia model in SD rats, ADC and CBF viability thresholds have been established and validated in previous studies in our laboratory.^{9,10} These thresholds were used to identify all pixels with abnormal ADC or CBF characteristics on each of the 8 imaged slices at each time point in both the SD and the WK group. The corresponding ADC and CBF lesion volumes were then calculated by summing the abnormal area and multiplying by the slice

Physiological Data (Mean±Standard Deviation)

	Baseline	1 h	2 h	3 h	4 h
WK					
MAPB, mm Hg	95±13	89±12	94±14	87±15	94±13
HR	389±31	381±26	386±35	379±26	392±30
Temp, °C	36.7±0.3	36.9±0.2	36.7±0.4	36.8±0.2	37.0±0.3
pO_2 , mm Hg	85±5				83±7
pCO_2 , mm Hg	43±5				39±4
pH	7.40±0.04				7.39±0.05
Glucose, mg/dL	169±31				148±29
SD					
MAPB, mm Hg	91±13	95±12	90±12	88±13	93±13
HR	381±27	390±25	380±25	382±30	391±28
Temp, °C	36.7±0.3	36.8±0.2	37.1±0.3	36.9±0.2	36.8±0.3
pO_2 , mm Hg	84±7				87±7
pCO_2 , mm Hg	39±6				37±5
pH	7.38±0.03				7.38±0.04
Glucose, mg/dL	156±23				143±21

MABP indicates mean arterial blood pressure; HR, heart rate; Temp, rectal body temperature.

thickness. The viability thresholds were 0.53×10^{-3} mm²/s for ADC and 0.30 mL/g/min for CBF.¹⁰

The time course of quantitative ADC and CBF values of the total ischemic right hemisphere (RH) and the normal left (LH) hemisphere were analyzed in both groups. In addition, region-of-interest (ROI, 4×4 pixels) analysis was performed in the lateral caudoputamen and the parietal cortex at the level of the optic chiasm (slice 4).

Pixel-by-Pixel Analysis

The ADC–CBF relationship over time was analyzed on a pixel-by-pixel basis. Pixel-by-pixel ADC–CBF scatterplots were performed at each time point, and the temporal evolution of ADC characteristics for different degrees of CBF reduction was evaluated for both groups. On the initial CBF map (45 min), CBF reduction in the RH was classified as follows¹²: (1) severe (<20% of the normal LH, “core CBF”), (2) moderate (21 to 40% of the LH, “penumbral CBF”), and (3) modest (41 to 55% of the LH). Subsequent ADC values of each cluster were then prospectively measured at each time point.

Statistical Analysis

Data are expressed as means±standard deviation. Sequential changes within the groups were statistically evaluated by ANOVA for repeated measures. An unpaired *t* test was used to compare intergroup or interhemisphere differences. Linear regression analysis was performed to correlate the ADC- and CBF-derived lesion volumes with TTC-defined infarct volumes. A 2-tailed value of $P < 0.05$ was considered significant.

Results

Physiological variables are shown in Table 1. All data were within the normal range and did not vary significantly between the 2 groups or at different time points ($P > 0.05$). Figure 1 shows representative ADC and CBF maps of 1 WK and 1 SD rat subjected to permanent MCAO.

Evolution of Cerebral Blood Flow-Derived Lesion Volume

The CBF-derived lesion volumes remained relatively constant throughout the study, and the lesion volumes at each

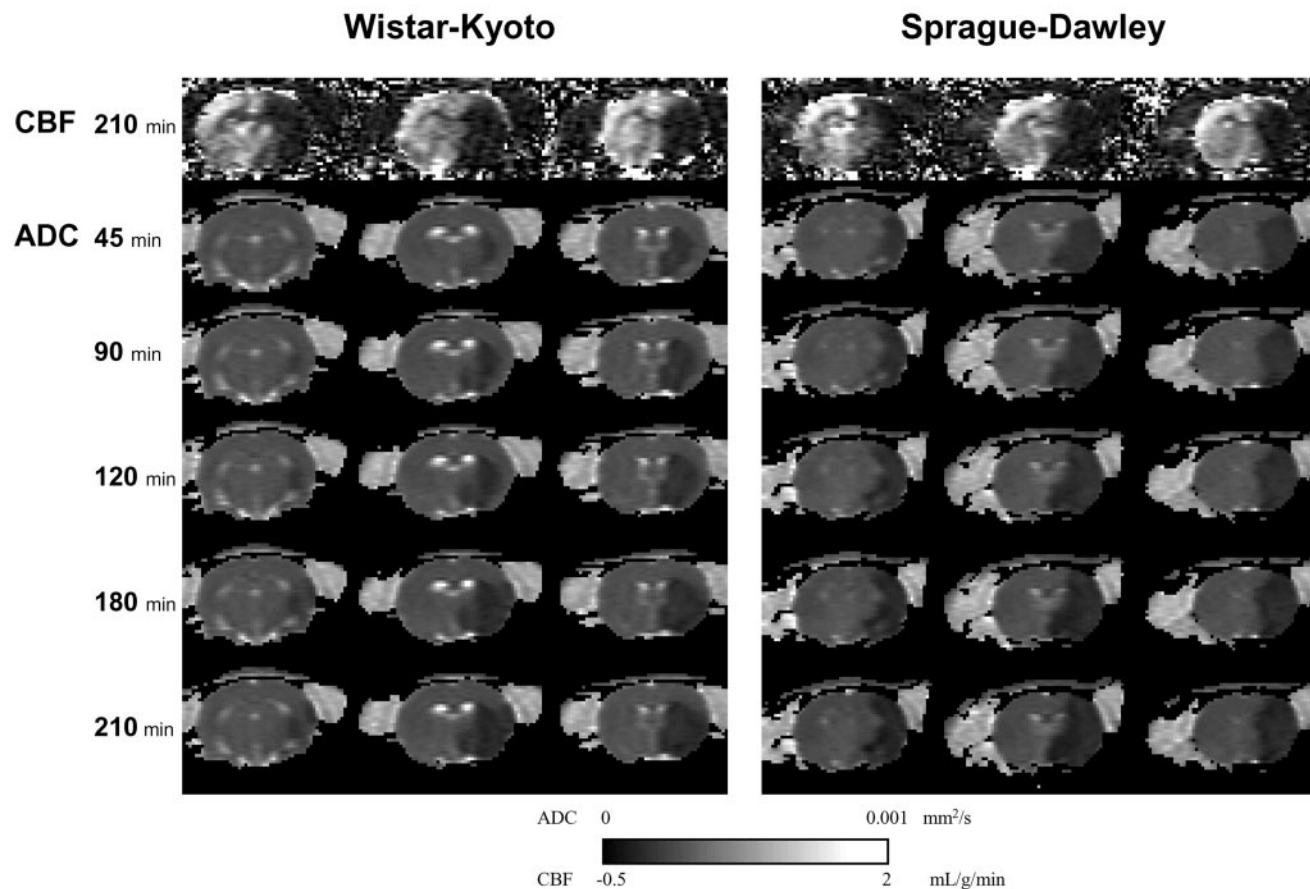


Figure 1. Representative ADC and CBF maps from one WK and one SD rat. Three of 8 maps are shown at 45, 90, 120, 180, and 210 min after occlusion for ADC maps and at 210 min for CBF maps.

time point were highly correlated with the TTC-defined infarct volume at 24 hours after MCAO for both the SD group (correlation coefficient r ranging from 0.93 to 0.97, $P < 0.001$ each) and the WK group (r ranging from 0.92 to 0.96, $P < 0.001$ each, Figure 2). The differences in abnormal perfusion volumes between rat strains were not statistically significant ($P = 0.08, 0.09, 0.07, 0.07,$ and 0.06 at 45, 90, 120, 180, and 210 min after MCAO). The mean TTC-defined infarct volume in SD rats was larger compared with that in WK rats, with an extent similar to that observed in the differences in CBF lesion volumes (266 ± 42 vs 233 ± 43 mm³, $P = 0.10$, Figure 2).

Evolution of ADC-Derived Lesion Volumes

The temporal evolution of the ADC-derived lesion volumes differed significantly between the 2 groups (Figure 2), because the ADC lesion in WK rats was significantly smaller at all time points ($P < 0.05$ each). In SD rats, the ADC lesion increased only slightly between 120 and 180 min (P for difference = 0.38 by ANOVA) and stopped growing after 180 min (P for difference between 180 and 210 min = 0.89), whereas the ADC lesion in the WK group continued to increase progressively between 120 and 210 min after occlusion. The increase was significant between 120 and 180 min ($P = 0.04$), but not between 180 and 210 min ($P = 0.06$). In SD rats, the ADC lesion volumes at 180 and 210 min were essentially identical with the TTC infarct volume 24 hours

after occlusion ($r = 0.97$, $P < 0.001$). In WK rats, in contrast, the ADC lesion at 210 min was smaller than the TTC infarct volume (211 ± 55 vs 233 ± 43 mm³, $P > 0.05$).

Evolution of the Diffusion/Perfusion Mismatch

The diffusion/perfusion mismatch region was identified as the difference between the abnormal perfusion and diffusion regions. In the WK group, the abnormal perfusion volume was significantly larger than the abnormal diffusion volume up to 90 min ($P < 0.001$) after MCAO. In the SD group, the difference between the abnormal perfusion and diffusion regions was only significant at 45 min ($P < 0.001$). The diffusion/perfusion mismatch volume gradually decreased over time in both groups, but it was significantly larger ($P < 0.05$) in WK rats up to 180 min after occlusion (Figure 3). By 210 min, the abnormal diffusion volume was 98% of the abnormal perfusion volume in SD rats and only 88% of the CBF lesion in WK rats, suggesting a persistent, although not significant, diffusion/perfusion mismatch.

Quantitative ADC and Cerebral Blood Flow Values

In the nonischemic LH, CBF and ADC values were stable across all time points and were not statistically different between groups. The average CBF and ADC values were 1.12 ± 0.21 mL/g/min and $0.75 \pm 0.03 \times 10^{-3}$ mm²/s for the WK group and 1.15 ± 0.25 mL/g/min and $0.76 \pm 0.03 \times 10^{-3}$ mm²/s for the SD

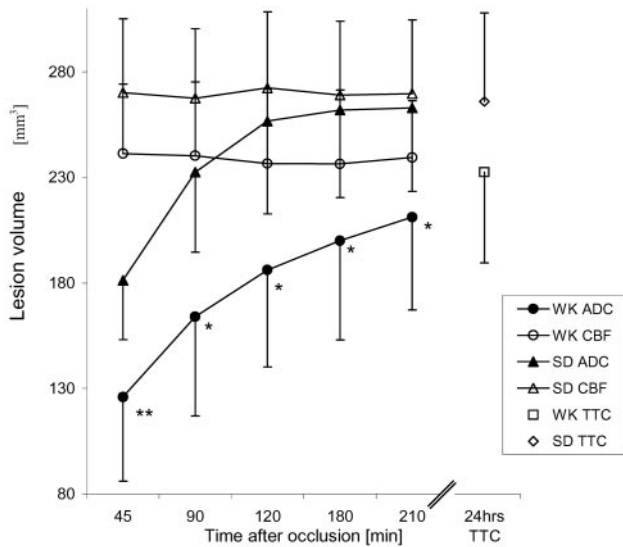


Figure 2. Temporal evolution of ADC- and CBF-derived lesion volumes (mean \pm standard deviation) by using previously established viability thresholds in permanently occluded rats. SD: open triangles indicate CBF lesion; closed triangles, ADC lesion; WK: open circles indicate CBF lesion; closed circles, ADC lesion. * $P < 0.05$, ** $P < 0.01$ for differences in ADC lesion volumes at the same time points.

group. There were also no differences between rat strains when region-specific CBF and ADC values in the lateral caudoputamen and the parietal cortex of the normal LH were analyzed (data not shown).

In the ischemic RH, no significant differences in the time course of region-specific and hemispheric CBF were observed between WK and SD rats (Figure 4A).

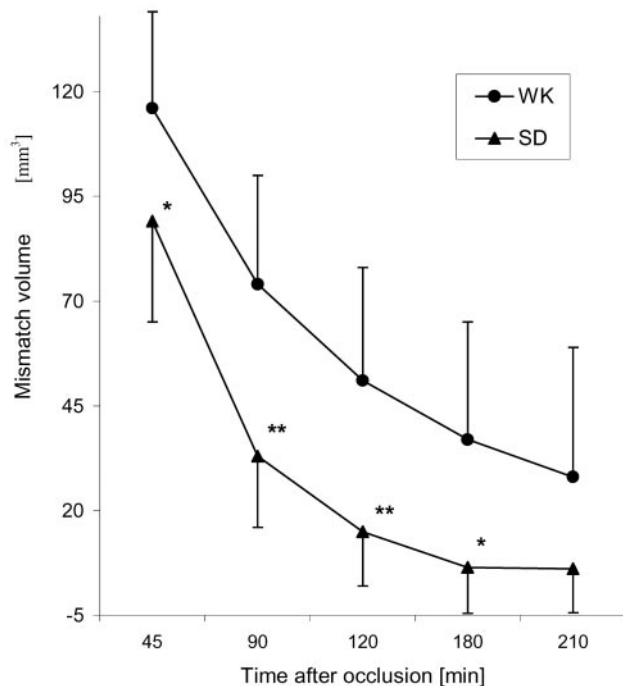


Figure 3. Temporal evolution of the diffusion/perfusion mismatch (mean \pm standard deviation). Triangles indicate SD; circles, WK. * $P < 0.05$, ** $P < 0.01$ for differences in diffusion/perfusion mismatch volumes at the same time points.

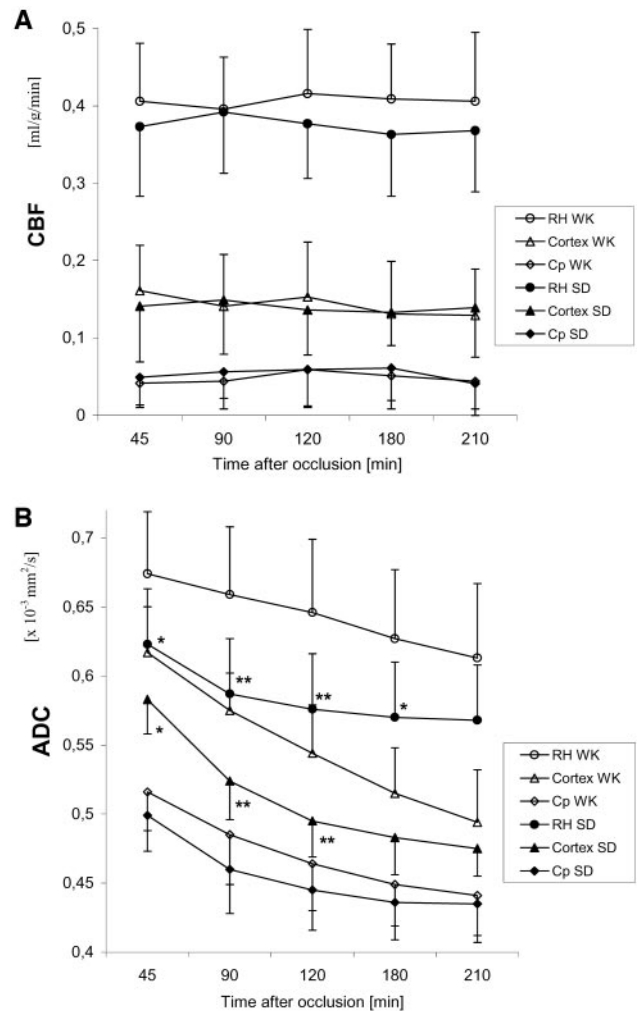


Figure 4. Time course of quantitative cerebral blood flow (A) and ADC (B) in the total right hemisphere (RH), the lateral caudoputamen (Cp), and the parietal cortex (Cortex). SD: closed circles indicate RH; closed diamonds, lateral caudoputamen; closed triangles, parietal cortex; WK: open circles indicate RH; open diamonds, lateral caudoputamen; open triangles, parietal cortex. * $P < 0.05$, ** $P < 0.01$ for differences in the same region of interest at the same time points.

Mean ADC values of the total ischemic RH were significantly lower in the SD group up to 180 min ($P < 0.05$) compared with those in the WK-group (Figure 4B). Although the ADC decreased more continuously over the entire observation period in WK rats, the decline in ADC values in SD rats was more pronounced within the first 120 min after occlusion, reflecting the rapid increase in ADC-derived lesion volume during the first 2 hours (Figure 2). In the ischemic parietal cortex, mean ADC was significantly higher in WK rats up to 120 min after MCAO ($P < 0.05$ each), whereas the intergroup differences in ADC values in the lateral caudoputamen were not significant at any time point.

Pixel-by-Pixel Analysis

Figure 5 shows the temporal evolution of ADC characteristics for different CBF-defined clusters. In tissues with severely reduced CBF ($< 20\%$ of normal LH), the mean ADC values in WK rats were significantly higher at all time points

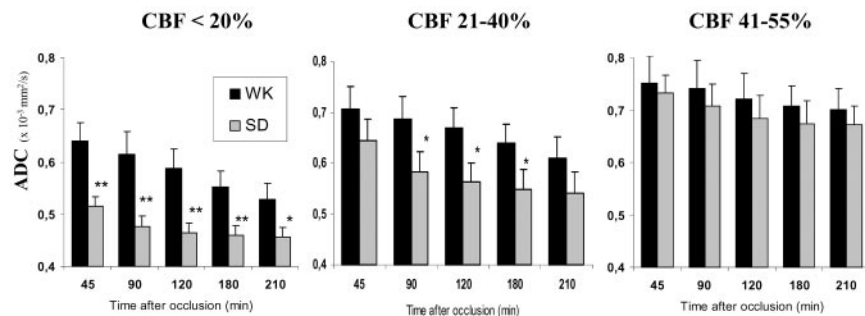


Figure 5. Temporal evolution of ADC values (mean \pm standard deviation) for pixels with severe (<20% of normal left hemisphere [LH]), moderate (21–40% of LH), and modest (41–55% of LH) cerebral blood flow reduction. Gray columns indicate SD; black columns, WK. * $P < 0.05$, ** $P < 0.005$ for differences in ADC at the same time points.

compared with those in SD rats ($P < 0.005$ up to 180 min, $P < 0.05$ at 210 min). While the ADC was only reduced to subnormal levels at 45 min and then gradually decreased over time in the WK group, the ADC in the SD group was severely reduced (below the viability threshold) at all time points. Similarly, in pixels with moderate degree of CBF reduction, the ADC in WK animals was persistently higher compared with that in SD animals. The difference in mean ADC values was significant at 90, 120, and 180 min after occlusion ($P < 0.05$). In tissues with only modestly reduced (41 to 55% of LH) CBF levels, ADC characteristics did not differ significantly between the 2 rat strains ($P > 0.05$).

Discussion

Several studies have reported differences in the extent of final infarct size among rat strains.^{2,5,13} However, the spatiotemporal evolution of the ischemic lesion during the acute phase after occlusion has not yet been investigated.

In the present study, the suture occlusion of the MCA resulted in consistently larger abnormal perfusion volumes in SD rats compared with WK rats, although the differences were statistically not significant. It has been postulated that there is a critical CBF threshold below which ischemic tissue is destined to become infarcted.^{8,14} We showed that the previously determined CBF viability threshold¹⁰ accurately predicted the extent of final infarct size in this permanent ischemia model for both SD and WK rats as demonstrated by the high correlation between abnormal perfusion volumes at all time points and the postmortem infarct size for both groups. However, the reasons for the interstrain variation in the extent of CBF deficit remain unclear. Parameters known to influence CBF such as type and degree of anesthesia, arterial blood pressure, blood gases, and body temperature are unlikely to attribute to this effect, because these variables did not differ between strains in this study. Variations in CBF are also not likely to explain these findings, because no differences in total or region-specific CBF of the normal left hemisphere were observed. Possibly, differences in the extent of the MCA territory, variability in vascular branching patterns, or differences in the collateral blood supply to the MCA distribution^{5,15,16} may account for variations in abnormal perfusion volumes.

The spatiotemporal evolution of the ADC-derived lesion volume differed significantly between the 2 rat strains. Although the abnormal diffusion volume in SD rats rapidly increased within the first 120 min and essentially stopped growing at 3 hours after MCAO, the ADC-derived lesion

volume was persistently smaller in WK rats and increased progressively over the entire 210-min imaging period. These differences in ADC lesion evolution cannot be simply explained by the constant differences in CBF lesion volumes. The magnitude of statistical interstrain differences in ADC lesions was more robust and variable compared with relatively stable differences in CBF lesions throughout the study. Moreover, although the ADC lesion volume maximized at 3 hours after MCAO in SD rats and virtually matched the TTC defined infarct size at 24 hours, the ADC lesion in WK rats further increased after 3 hours without reaching the final TTC infarct volume even at 210 min after occlusion.

We analyzed the time course of CBF and ADC in 2 brain regions that are typically involved with ischemic injury in this stroke model.¹⁷ Although the ADC decrease in the parietal cortex was more pronounced in SD rats with significant differences compared with that in WK rats up to 2 hours after MCAO, the CBF reduction was comparable between groups, indicating that the degree of CBF reduction was likely not a major limiting factor responsible for the differences in ADC decline. Furthermore, the pixel-by-pixel ADC-CBF scatterplots analysis revealed significant interstrain differences in ADC dynamics for pixels with the same extent of CBF reduction. In ischemic tissue with severely reduced (<20% of normal values) and moderately reduced (21 to 40% of normal) CBF levels, the ADC decrease over time was slower and less robust in WK rats compared with that in SD rats, whereas pixels with only modestly reduced CBF (41 to 55% of normal) did not show significant interstrain differences in ADC characteristics. These findings suggest that SD rats exhibit increased susceptibility to a similar degree of reduced blood flow, resulting in a more rapid progression of ischemic damage as measured by the extent of diffusion imaging lesions compared with WK rats. Importantly, the CBF threshold associated with infarction, ie, 0.3 mL/g/min, is comparable between the 2 rat strains, as indicated by the good correlation between CBF-derived lesions and TTC infarct for both rat strains.

This study demonstrated substantial interstrain differences in the temporal evolution of the diffusion/perfusion mismatch. The mismatch region in WK rats was markedly larger up to 3 hours after MCAO compared with that in SD rats. Moreover, whereas the volume of the diffusion/perfusion mismatch was significant up to 90 min after occlusion in WK rats, the difference between abnormal diffusion and perfusion volume was only significant at the 45-min time point in SD rats. The diffusion/perfusion mismatch provides a volumetric

estimate of the putative ischemic penumbra and the duration of its temporal existence and is thought to represent potentially salvageable ischemic tissue, and is thus a major target for acute stroke therapies.⁶ Therefore, interstrain differences in the temporal evolution of the diffusion/perfusion mismatch may result in different therapeutic time windows for the same drug. In various stroke studies using the rat MCAO model, the potential to reduce infarct size with neuroprotective therapies such as NMDA or calcium antagonists^{4,7} or hypothermia¹⁸ was reported to depend on the rat strain used. Interstrain differences in mismatch evolution in the acute phase of ischemia as well as differences in resistance to moderately and severely depressed blood flow, as observed in the present study, may explain some of these interstrain discrepancies in drug efficiency.

In conclusion, quantitative diffusion and perfusion imaging during the acute phase after permanent suture MCAO demonstrated substantial differences in the temporal evolution of the ischemic lesion, and the putative penumbra between WK and SD rats. Because this stroke model in rats is commonly used to study the effects of novel therapeutic approaches, these interstrain variations must be taken into account to properly evaluate the results of new therapies on lesion development.

References

1. Laing RJ, Jakubowski J, Laing RW. Middle cerebral artery occlusion without craniectomy in rats. Which method works best? *Stroke*. 1993;24:294–297.
2. Aspey BS, Cohen S, Patel Y, Terruli M, Harrison MJ. Middle cerebral artery occlusion in the rat: consistent protocol for a model of stroke. *Neuropathol Appl Neurobiol*. 1998;24:487–497.
3. Kuge Y, Minematsu K, Yamaguchi T, Miyake Y. Nylon monofilament for intraluminal middle cerebral artery occlusion in rats. *Stroke*. 1995;26:1655–1657.
4. Oliff HS, Marek P, Miyazaki B, Weber E. The neuroprotective efficacy of MK-801 in focal cerebral ischemia varies with rat strain and vendor. *Brain Res*. 1996;731:208–212.
5. Oliff HS, Coyle P, Weber E. Rat strain and vendor differences in collateral anastomoses. *J Cereb Blood Flow Metab*. 1997;17:571–578.
6. Schlaug G, Benfield A, Baird AE, Siewert B, Lovblad KO, Parker RA, Edelman RR, Warach S. The ischemic penumbra: operationally defined by diffusion and perfusion MRI. *Neurology*. 1999;53:1528–1537.
7. Sauter A, Rudin M. Strain-dependent drug effects in rat middle cerebral artery occlusion model of stroke. *J Pharmacol Exp Ther*. 1995;274:1008–1013.
8. Hoehn-Berlage M, Norris DG, Kohno K, Mies G, Leibfritz D, Hossmann KA. Evolution of regional changes in apparent diffusion coefficient during focal ischemia of rat brain: the relationship of quantitative diffusion NMR imaging to reduction in cerebral blood flow and metabolic disturbances. *J Cereb Blood Flow Metab*. 1995;15:1002–1011.
9. Shen Q, Meng X, Fisher M, Sotak CH, Duong TQ. Pixel-by-pixel spatiotemporal progression of focal ischemia derived using quantitative perfusion and diffusion imaging. *J Cereb Blood Flow Metab*. 2003;23:1479–1488.
10. Meng X, Fisher M, Shen Q, Sotak CH, Duong TQ. Characterizing the diffusion/perfusion mismatch in experimental focal cerebral ischemia. *Ann Neurol*. 2004;55:207–212.
11. Strupp JP. Stimulate: a GUI based fMRI analysis software package. *Neuroimage*. 1996;3:S306. [Abstract].
12. Ginsberg MD. Adventures in the pathophysiology of brain ischemia: penumbra, gene expression, neuroprotection: the 2002 Thomas Willis Lecture. *Stroke*. 2003;34:214–223.
13. Duverger D, MacKenzie ET. The quantification of cerebral infarction following focal ischemia in the rat: influence of strain, arterial pressure, blood glucose concentration, and age. *J Cereb Blood Flow Metab*. 1988;8:449–461.
14. Kohno K, Hoehn-Berlage M, Mies G, Back T, Hossmann KA. Relationship between diffusion-weighted MR images, cerebral blood flow, and energy state in experimental brain infarction. *Magn Reson Imaging*. 1995;13:73–80.
15. Herz RC, Jonker M, Verheul HB, Hillen B, Versteeg DH, de Wildt DJ. Middle cerebral artery occlusion in Wistar and Fischer-344 rats: functional and morphological assessment of the model. *J Cereb Blood Flow Metab*. 1996;16:296–302.
16. Fox G, Gallacher D, Shevde S, Loftus J, Swayne G. Anatomic variation of the middle cerebral artery in the Sprague-Dawley rat. *Stroke*. 1993;24:2087–2092.
17. Reith W, Hasegawa Y, Latour LL, Dardzinski BJ, Sotak CH, Fisher M. Multislice diffusion mapping for 3-D evolution of cerebral ischemia in a rat stroke model. *Neurology*. 1995;45:172–177.
18. Ren Y, Hashimoto M, Pulsinelli WA, Nowak TS Jr. Hypothermic protection in rat focal ischemia models: strain differences and relevance to 'reperfusion injury.' *J Cereb Blood Flow Metab*. 2003;24:42–53.